DETERMINATION OF ATMOSPHERIC PARAMETERS OF T TAURI STARS

R. Piorno Schiavon[1,2], C. Batalha[1], B. Barbuy[2]

1 Observatório Nacional, Departamento de Astrofísica

Rua General José Cristino, 77, São Cristóvão

20921-400 Rio de Janeiro, Brazil

2 Universidade de São Paulo, IAG, Departamento de Astronomia

C.P. 9638, São Paulo 01065-970, Brazil

1

ABSTRACT. The inferred effective temperatures (T_{eff}) and surface gravities of T Tauri stars (TTS) are usually contaminated by the presence of a non stellar continuum emission (veiling) and the strong chromospheric activity characteristic of these objects. In this work, we develop a method to determine T_{eff}'s and surface gravities ($\log g$) of a group of TTS. This method is based on the comparison between observed and theoretical molecular and atomic line depth ratios being therefore insensitive to the influence of veiling. We show the strong dependence of our line depth ratios upon gravity and temperature. The resulting gravities, as expected for TTS, average between the values of dwarf and giant stars. Previously published gravities for each of our stars vary widely due in part to the differences in the adopted visual extinction, veiling (if ever considered) and methods of assessing the stellar luminosity. Our values of T_{eff} and $\log g$ have the uniqueness of being entirely derived from high resolution data and are not affected by circumstellar extinction or veiling when line ratios are used. They therefore serve as more reliable input parameters for future spectral synthesis analyses of T Tauri Stars requiring model atmospheres. We provide a table relating theoretical line depth ratio with T_{eff} and $\log g$ for easy assessment of TTS fundamental parameters.

Key words: T Tauri stars, molecular lines, synthetic spectra

1. INTRODUCTION

Reliable atmospheric parameters of T Tauri stars (TTS) provide the cornerstone in understanding the formation and pre main sequence evolution of low mass stars as they contract towards the zero age main sequence. Without the basic information of effective temperatures (T_{eff}) and surface gravities ($\log g$), the accurate determination of the elemental atmospheric abundances of TTS is likely to result in failure.

The present picture of a classical T Tauri star (CTTS) consists of a central star surrounded by an optically thick accreting disk rotating at about the stellar equatorial plane. First attempts to model this system were made by Hartmann & Kenyon (1987) and Bertout, Basri & Bouvier (1988), in which a shear boundary layer interfacing the stellar photosphere and the disk produces the continuum veiling and part of the broad lines typical of these stars. In more recent approaches, the magnetosphere has an active role in shaping the circumstellar environment. Depending on the strength of the stellar magnetic field lines, the disk may never reach the star, being disrupted at about the corotational radius (Königl 1991, Shu et al. 1994, Kenyon et al. 1994). In this case, the disk matter is funneled along the magnetic field lines to the stellar surface, generating hot gas at the footpoints of the magnetic columns.

Owing to the above mentioned phenomena, the spectrum of a CTTS is usually very complex and its main features are: *i)* infrared (IR) and radio flux excesses, which are largely believed to be disk emission; *ii)* optical and ultraviolet excesses which correlate with the IR fluxes (Bertout 1989, Hartigan et al. 1990). This nonstellar continuum radiation in the optical range reduces the depth of photospheric absorption lines and is the main source of the so called veiling (Basri & Batalha 1990, Hartigan et al. 1991); *iii)* chromospheric filling in of selective absorption lines, which constitutes a small fraction of the veiling. This property is well correlated with stellar activity (Finkenzeller & Basri 1987). Further indications of stellar activity are the *iv)* X-ray emission, probably due to hot solar-type coronae and *v)* the periodical photometric variability suggesting the transit of bright and dark spots on the stellar atmosphere (Bouvier 1990). *vi)* The upper Balmer series are in emission indicating mass transport in the stellar surroundings. *vii)* Forbidden lines are present and their total flux correlates with the IR luminosity (Cabrit et al. 1990).

The so called weak T Tauri stars (WTTS) differ from the CTTS in their observed characteristics, presenting much milder near IR and blue color excesses (if any), no forbidden line emission (Edwards et al. 1994), the absence of a Balmer jump as well as Balmer line emission (Valenti, Basri & Johns 1993). The current interpretation of these features is the lack of accreting disks around the WTTS.

The application of canonical methods to determine the atmospheric parameters of CTTS is largely prohibited by the above spectral features, although they might be effective if applied to WTTS. First of all, color indices are severely changed by the λ-dependent nonstellar emission and circumstellar extinction, misleading any of the classical attempts to infer T_{eff} or metallicities from the usual photometric indicators. Moreover, the optical veiling and probably the chromospheric filling in reshape the wings of moderate to strong lines inhibiting the use of the synthetic profile technique to derive the stellar T_{eff}. The same argument can be presented against using the classical curve of growth method to analyze the properties of CTTS. The determination of TTS surface gravities from their locus on the theoretical HR-diagram is strongly affected by the errors in luminosity, temperature and the uncertainties on the pre-main-sequence evolutionary tracks.

Recently, however, this situation has begun to change as more analyses based on high resolution data have been presented. High resolution and high S/N spectroscopy has allowed direct measurements of the intrinsic stellar luminosity, after proper veiling correction are carried out (Hartigan et al. 1989, Basri & Batalha 1990 and Hartigan et al. 1991). This is done by comparing the TTS spectrum with that of a template star and analyzing the residuals. Implicitly, it is assumed that both stars share similar atmospheric parameters,

metallicity and chromospheric activity.

Theoretical analyses of the underlying photospheres have been made by Calvet, Basri & Kuhi (1984) and Calvet & Marin (1987). In these works, the absorption spectra of classical TTS are synthesized using a simplified NLTE treatment. The temperature minimum and the associated gas column density are the key parameters in matching the observations. The curve of growth method has also been successfully applied to Sz 19 and its fundamental stellar parameters have been derived (Franchini et al. 1991). In these studies, the veiling as an external source of continuum emission has not been considered because of the intrinsic theoretical approach and because the star lacks veiling. Specific studies of atmospheric features where consistent veiling corrections are carried out are also being released. Basri, Martin & Bertout (1991) derive lithium abundances for a large sample of TTS and find abnormally large values of N_{Li} (> 3.3) for some of the stars. They suggest that the overabundance might be the result of errors in the ascribed stellar parameters. Magazzù, Rebolo & Pavlenko (1992) found that Li abundances are reduced, on the average, when NLTE effects are taken into account. Nevertheless, some of their stars still remain overabundant in Li. Martin et al. (1994) performed NLTE analyses of more than 50 WTTS and found no Li overabundances. They conclude that the overabundances found in CTTS may be attributted to the errors in the input atmospheric parameters. Thus, an accurate method to determine CTTS atmospheric parameters can help to resolve the Li problem in TTS.

Batalha & Basri (1993) and Batalha et al. (1995) attempt to model the infrared triplet lines of CaII and verify the conditions of their forming regions. They find that disk accretion, as indicated by the near IR excess, Hα fluxes and veiling, does correlate with the chromospheric line strengths of CaII and HeI at 5876 Å. The connection is conspicuous and suggests that accretion – probably combined with stellar magnetic field lines – induces regions on the stellar surface with a distribution of gas density and temperature similar to those of solar type magnetically active regions. Chromospheric lines are therefore enhanced in classical TTS.

In this paper we investigate the photospheres of TTS, largely exploring the technique of line depth ratios (LDR's). Gray & Johanson (1991) devised a method to determine T_{eff} based on the strong correlation with the LDR of atomic lines, presenting an opposite response to the increase of T_{eff}. The application of this method to very active stars is not free from drawbacks since the selective chromospheric filling in and the strong spotting can mask the actual dependence of line depths with T_{eff}. The filling in can be avoided by a careful selection of the pair of lines among those free from chromospheric contamination (Finkenzeller & Basri 1987). The effect of cool spots on line absorption intensities is negligible for lines sensitive to temperature such as the LiI resonance line at $\lambda 6708$ Å (Pallavicini et al. 1993) and CaH

4

rotational lines (Barbuy et al. 1993, Paper I), at least for the typical TTS surface coverage by spots. Therefore, we import the LDR technique developed by Gray & Johanson (1991), and apply to several TTS (Basri & Batalha 1990), to permit preliminary assessment of the intrinsic stellar colors. The derived stellar parameters are used as an input to synthesize selected spectral regions. We verify that the LDR of a given pair of lines presents negligible changes if the spectrum is artificially veiled ($0 < v < 1.0$) or rotated ($0 < v\sin i < 20$ Km/s) by the values here reported. Therefore, we adopted LDR's instead of equivalent width ratios because the former are less sensitive to spectral noise than the latter.

Since the TTS are undergoing contraction towards the main sequence, their surface gravities are expected to be lower than those characteristic of dwarf stars. In fact, Mould & Wallis (1977), using photometry of the 6830 Å CaH band, concluded that TTS have surface gravities averaging between dwarf and giant values. The results of Mould & Wallis have been confirmed since more accurate values of surface gravity based on improved TTS stellar luminosities have been determined (see Strom et al. 1989, Cohen, Emerson & Beichman 1988, Cabrit et al. 1990, Hartmann & Kenyon 1990 and Hartigan et al. 1991). In the present work, we explore the use of molecular lines in high resolution data to better constrain the TTS gravities.

We determine T_{eff} for 13 TTS, most of them belonging to the Taurus-Aurigae stellar formation complex. We successfuly determine surface gravities for the cooler stars using spectral synthesis of CaH and atomic lines. In section 2, we briefly present the observations, data analysis and T_{eff} determinations based upon published calibrated main sequence data. In section 3, we describe the synthesis and the computation procedure to achieve the T_{eff} and $\log g$. A brief summary is presented in section 4.

2. OBSERVATIONS AND DATA ANALYSIS

The observations used in this paper result from an extensive observational program undertaken at Lick Observatory by Dr. Gibor Basri and collaborators, between 1986 October and 1989 October. This program includes the observation of the brighter objects in the Taurus-Auriga complex with the Hamilton-Echelle Spectrograph, aiming to study the strong emission lines of TTS. The detector used was a TI 800×800 CCD chip. The list of TTS studied in our work is given in Table 1. Some details of the spectral reduction procedure are described by Basri, Wilcots & Stout (1989) and Basri & Batalha (1990). The average S/N of the spectra is about 80.

The total echelle region runs from about 5500 to 9000 Å with gaps in between orders. Those gaps result from the fact that the CCD used in the observations is smaller than the format of the Hamilton-Echelle spectrograph, so that there are cutoffs in the spectral coverage between consecutive orders.

We select the following spectral sub-regions: $\lambda\lambda 5700$-5710 Å which contains the atomic lines used in the $T_{\rm eff}$ determination; $\lambda\lambda 6770$-6820 Å containing some of the most conspicuous CaH lines found in the sunspot spectrum (Boyer et al. 1975, 1976, 1978 and 1982) and $\lambda\lambda 5400$-6400 Å which is used in the veiling measurements (see below).

We also use spectra of a number of template stars from the Hyades and the field. These stars are listed in Table 2. They were observed with the same instrumental apparatus as the TTS. The S/N of the template star spectra is typically around 200.

Continuum normalization was made using IRAF package routines. The procedure consists of fitting a spline curve on selected continuum windows of the given echelle order and then dividing the spectrum of this order by the fitted curve. In some cases we did not find a unique solution that satisfactorily fit the whole order. In such cases, we fit different curves for the intervals $\lambda\lambda 6770 - 6790$Å and $\lambda\lambda 6790 - 6810$Å.

Gravities for three stars are derived by fitting directly CaH molecular lines. Therefore, we have to subtract the continuum nonstellar contribution from the observed spectrum. The continuum veiling is expected to be fairly constant redward of 5500 Å (Basri & Batalha 1990). Hence, we extract the veiling by applying the simple expression

$$F_{ph} = (1 + v)F_{TT} - v,$$

where F_{TT} is the observed TTS profile, relative to a normalized continuum. It is the sum of the fluxes originating in distinct emitting regions. F_{ph} is the normalized photospheric flux and v is the continuum veiling, which is the total non stellar continuum in units of F_{ph}.

The v-parameter can be determined from its influence on absorption line depths. Basri & Batalha (1990) performed such an analysis using the same spectral database of this work, but in some cases adopting different spectral types. We adopt their values for every star whose spectral type coincides with ours. For the other stars, we determine independent values, comparing the depths of weak unblended atomic lines between the TTS spectra and those of Hyades templates. The values are shown in column 7 of Table 1.

2.1 Calibration of $T_{\rm eff}$

Effective temperatures of T Tauri Stars are usually estimated from their spectral types and the calibration of Cohen & Kuhi (1979) is the most widely adopted. Therefore, it is not surprising to find a general agreement among the temperatures of several CTTS although the systematic errors generated while translating spectral types to T_{eff} are not negligible for cool stars (de Jager & Nieuwenhuijzen 1987, Strom et al. 1988). In this work, we determine the T_{eff} of the program TTS using the LDR of two absorption lines with different temperature sensitivities. We first derive intrinsic colors from which we assess the T_{eff}, using a calibration from the literature.

We carried out a survey of line pairs close in wavelength and free from strong blends or telluric features. We ended with the following lines: $\lambda\lambda$ (Å) ScI-CuI 5700.2/FeI 5706.1 VI 5703.6/FeI 5706.1, VI 5707.0/FeI 5706.0 and FeI 6200.3/ScI 6210.7 (Moore, Minnaert & Houtgast 1966). Further analysis led us to exclude some of these because of the possibility that they are filled in by chromospheric emission. Finally, we selected the pair VI 570.7/570.6, which is shown in Table 3 together with the atomic parameters. These lines happen to be the same set previously used by Basri & Batalha (1990) to infer TTS spectral types. Their inverse sensitivity to temperature is illustrated in Figure 1 where we plot the spectra of two Hyades stars with different spectral types. The line pair of Gray & Johanson (1991) is located in one of the gaps of our echelle setting and therefore, it could not be included in our study.

We measure the LDR VI 5707/FeI 5706 for a set of field stars and cool members of the Hyades cluster, with available photometry (see Table 2). We fit gaussians to the line profiles and take the amplitude of the curve as the measured line depth. The LDR for each star is given in Table 2. The (R–I) color indices of these stars are taken from Upgren (1974) (Hyades) and Gliese (1969) (field stars) and they are all in the Kron system. In Figure 2 we present the observed LDR $vs.$ (R–I)$_0$ relation. A larger number of template stars would statistically improve our relation, especially at the cool end. We include in section 3.2 the rotational lines of CaH to compute the fundamental parameters of stars cooler than 4500 K. A quadratic polynomial with coefficients $(a_0, a_1, a_2) = $ (-0.10901979, 0.58777191, -0.10085137) is then fit to the relation of Figure 2. The intrinsic T Tauri (R–I)$_0$ colors are then computed using this polynomial fit and the TTS LDR's.

The TTS LDR's are measured using the same procedure described above. Given the S/N ratio of our spectra (see Table 1), the average formal error in the LDR's due to continuum normalization procedures is equal to 0.04 for the TTS and 0.01 for the template stars. The average error induced by the gaussian fitting is equal to 0.06. Therefore, the final average error in our LDR's is about 0.07 for the TTS and 0.06 for the templates.

We have observations taken during different seasons for AA, BP, DF and DK Tau so that

we may check for variations of the LDR. The variations are smaller than the above mentioned error for all stars, except AA Tau. This will be briefly discussed in Section 3.2. For the other stars, we coadded the individual spectra in order to analyze average data, with improved S/N. The error in the TTS $(R–I)_0$ colors is about 0.03, based on the mean deviation of the points from the polynomial fit.

We did not derive colors for DE and DF Tau because their LDR's fall outside the range encompassed by the set of data assembled in Table 2 (they are much cooler than the template stars). The final color indices are presented in Table 4 with an average for those stars with more than one observation. These indices must be considered as first approximations to the real stellar values since, in our approach, we are deriving TTS stellar parameters by comparing them to those taken from a set of main sequence templates. As pointed out by Hartigan et al. (1991), the ideal set of templates to be used in a study of CTTS would be formed by a group of WTTS from the same parental cloud of the program stars and absent of any signature of disk accretion. Such stars, which are also undergoing contraction towards the ZAMS, would have slightly lower gravities and higher chromospheric activity than their stable main sequence counterparts. In addition, we would not expect severe metallicity differences between the template and program stars, since they are born out from the same interstellar material.

We rely upon the calibration of Soderblom et al. (1993) based on a set of 87 Pleiades stars to translate colors to effective temperatures. This cluster is a relatively young one (100 My), and the chromospheric activity of its stars is comparable to that of a weak T Tauri (Batalha et al. 1994). We fit a third degree polynomial with coefficientes $(a_0, a_1, a_2, a_3) =$ (6943.3565, -6651.5949, 1776.5984, 2290.4328) to this data, excluding few stars that deviate more than 3 times the nearby standard deviation. Effective temperatures of our templates and TTS are then calculated, and the final values are listed in Tables 2 and 4 respectively. We estimate an error of 100K in the inferred TTS effective temperatures by measuring the standard deviation of the residuals around the polynomial fit. However, this is a lower limit to the error, since systematic effects are not taken into account.

3. SPECTRUM SYNTHESIS

Atomic lines show different responses to changes in gravity. Therefore, dwarfs and giants of the same temperature might present different LDR's. The procedure described in the previous section to achieve effective temperatures will be reliable whenever the TTS is near the beginning of the ZAMS; otherwise, gravity effects must be taken into account in the

analysis of LDR's. We synthesize the pair of lines from which the TTS temperatures presented in Table 3 are derived and explore their response to gravity. The distinct behaviour of these lines allows us to make a first guess as to the gravity of individual stars. We verify these initial guesses of $\log g$ by synthesizing rotational lines of CaH.

3.1 Computation of atomic LDRs and first guess for $\log g$

We have built a theoretical relation between T_{eff} and LDR for the pair 570.7/570.6, computing synthetic spectra for a grid of model atmospheres. This grid is computed, with T_{eff} and $\log g$ ranging from 3600 to 5800K (steps of 200K) and 3.0 to 4.5 (steps of 0.5 dex) and solar metallicity. Each model atmosphere is interpolated in the grids of Kurucz (1992) and the synthetic spectrum is computed using the program described in Barbuy (1982). Gray (1994) points out that the trend of LDR versus T_{eff} might be dependent on metallicity whenever one of the lines is near saturation. However, Balachandran & Carr (1994) determined solar abundances for some TTS of the Taurus-Auriga cloud (UX Tau A and TAP 56) which supports our basic assumption of solar metallicity and the use of our calibration (see Figure 2) for pre-main-sequence stars.

In order to compute theoretical LDRs, we need the oscillator strengths (gf) of the involved lines. In the absence of laboratory determinations, we derive the gf values by fitting the spectra of standard stars. We make several tests before achieving the final gf values presented in Table 3. Both lines of the pair are blends, which decreases the accuracy of their determined oscillator strengths. The starting point in our search for the atomic gf factors is to fit the disk-integrated solar spectrum of Kurucz et al. (1984) using two different inputs: the theoretical model of Kurucz (1992) and the empirical model of Holweger & Müller (1974). We adopt $T_{\text{eff}}^{\odot}$ = 5780K and $\log g^{\odot}$ = 4.44. The two sets of gf values thus obtained are in perfect agreement. We also compute another set of gf values comparing the theoretical solar spectrum with the observed solar disk-center spectrum (Delbouille, Roland & Neven 1973). The set of gf values thus obtained is substantially different from the previous one. This is not surprising, since the solar disk center spectrum does not include the contribution of limb-darkened layers. Since we are applying these gf values to the synthesis of disk integrated stellar spectra, the best suited set is the one derived from the fit of the Kurucz et al. solar spectrum.

A drawback of semi-empirical gf values is that of being dependent on the chosen model atmosphere. Therefore, we verify our previous figures by matching the spectrum of a well known star, cooler than the Sun. We compute the synthetic spectrum of Arcturus (α Bootis, HD 124897), interpolating a model atmosphere with T_{eff} = 4340K, $\log g$ = 1.6 and [Fe/H] =

9

−0.81 (Bell, Edvardsson & Gustafsson 1985) in the grid of Kurucz model atmospheres. We fit the spectrum of the photometric atlas of Arcturus (Griffin 1969), but no set of *gf* values satisfies simultaneously the observed lines in the spectrum of the disk-integrated Sun and that of Arcturus. There are three points to be considered here. First, it is possible to use the asymmetries of the observed solar spectrum profiles in order to guess the *gf* values of individual blended lines which are washed out in the lower resolution, lower S/N spectrum of Arcturus. Secondly, the model atmospheres of Arcturus and the Sun are interpolated in the same grid and the disagreement may reflect errors in the assumed atmospheric parameters of Arcturus, since the solar ones are known with the highest accuracy. Thirdly, the metallicity diference between the Sun and Arcturus may be large enough that the saturation problems pointed out by Gray (1994) are important. Thus, we are more confident with the results based on the solar spectrum.

We use our set of templates as guidelines towards low $T_{\rm eff}$'s using the effective temperatures derived in Section 2.1. In this way, we try to match not the observed spectrum of each star, but the observed trend of the LDR as a function of $T_{\rm eff}$. In Figure 3, we plot the relation computed using the solar *gf*'s together with the positions of the Hyades and field stars in the LDR-$T_{\rm eff}$ plane. The location of the templates in Figure 3 lies at about the trend defined by the computed curves. Hence, the final *gf* values, listed in Table 3, are those which fit the line profiles in the solar spectrum and followed the expected trend towards low $T_{\rm eff}$'s. In every calculation we adopt an interaction constant of $C_6 = 3.0 \times 10^{-31}$ for all the lines.

The synthetic spectra range from 5705 to 5709 Å and are convolved with rotational profiles to simulate the typical *v*sin*i* of the program stars. The LDR's do not vary significantly for *v*sin*i* between 5 and 20 Km/s. We measure the depths of the lines in each theoretical spectrum and compute the final relations shown in Figure 3 for $\log g = 3.0$, 3.5, 4.0 and 4.5. In Table 5, we present several LDRs and their associated temperatures and gravities. The strong dependence of the LDR on $\log g$ at the cool end of Figure 3 is striking. This is because iron is predominantly neutral at low temperatures while vanadium is still partially ionized. Therefore, the intensity of the neutral iron line is a function of electronic pressure, while the intensity of the neutral vanadium line is not (Gray 1976, chap. 12), yielding, as a result, different responses to gravity at low temperatures. As the temperature increases, both elements become equally ionized, so that the intensity of the neutral lines stops being a function of eletronic pressure and the LDR is thus insensitive to gravity.

3.2 Computation of the CaH lines: Temperature and Gravity Determinations

10

The model computations of Section 3.1 show that the relation between the LDR and $T_{\rm eff}$ is degenerate, in the sense that, for one given LDR, we can have a number of $T_{\rm eff}$'s, depending on the gravity of the star (Figure 3). This effect is more important for stars cooler than 4500K. In order to remove this degeneracy, we need one more relation between LDR, $T_{\rm eff}$ and $\log g$. In Section 2, we used an empirical relation between LDR and $T_{\rm eff}$, which can only be applied to dwarf stars. In this Section, we explore the dependence of CaH lines on $T_{\rm eff}$ and $\log g$, with the aim of breaking this degeneracy.

CaH lines are present in the wavelength range $\lambda\lambda\,6100 - 7100$ Å. The $\lambda\lambda\,6770 - 6810$ Å region ended up to be the best suited for studies of CaH lines because of the weakness of CN and TiO molecular lines and the relatively low number of blended atomic lines. The region around 6390 Å could also be used, but, unfortunately, it falls within one of the gaps in the spectral coverage.

The spectral synthesis code and atomic plus molecular data used are described in Paper I, in which the CaH $B^2\Sigma - X^2\Sigma$ and $A^2\Pi - X^2\Sigma$ systems are studied. In that paper, the oscillator strengths for the two electronic transitions are chosen so that we could reproduce, on average, the observed high-resolution spectrum of a number of Hyades and field stars. Here, we redetermine these oscillator strengths, by fitting in a more rigorous way the spectra of two stars from the Hyades cluster, VA 404 and VA 622. The temperatures adopted here for these stars are more reliable than the values of Paper I. The $T_{\rm eff}$'s are taken from the Kron $(R-I)_0$ colors, as explained in Section 2.1 (Table 4), while the temperatures adopted in Paper I are derived from spectral types. The gravities are taken from the positions of these stars in Figure 2 (the two coolest stars); for VA 404, we have $\log g = 4.0$ and for VA 622, $\log g = 4.5$. The adopted model atmospheres are interpolated in the grids from Kurucz (1992) assuming solar metallicities. We derive $f_{el}^{A-X} = 1.2$ (0.5 in Paper I) and $f_{el}^{B-X} = 1.4$ from this analysis. The latter is less reliable, since it depends upon the fitting of fewer lines than the former. In Figure 4, we display the response of CaH lines to temperature, (for $\log g$ = 4.0) and gravity (for $T_{\rm eff} = 4000$ K).

Atomic neutral lines usually grow stronger towards low gravities because of the larger concentration of neutral metals at the same optical depth. Hydride lines behave in the opposite manner, because the formation of the ionic molecule tends to increase with increasing gas pressure as the star approaches the main sequence. Therefore, the (veiling independent) LDR between one CaH line and one atomic line is used here to further constrain the stellar parameters. If we model the dependence of this new LDR upon the stellar parameters, we will have the additional relation needed to break the degeneracy apparent in Figure 3. We synthesize the region between 6790 and 6810 Å and the best CaH line is chosen. We use

the line at 6796 Å, which shows a good response to $\log g$, is fairly deep and easily found in our set of CTTS spectra. Next, we compute two new LDR's, CaH 6796/FeI 5706 and CaH 6796/VI 5707, for the grid of model atmospheres referred to in Section 3.1. This gives us the theoretical dependence of the LDRs upon T_{eff} and $\log g$ (for solar metallicity). (See also the discussion of the VI 5707/FeI 5706 LDR in Section 3.1). The responses of the two new LDR's to T_{eff} and $\log g$ are very similar to each other. One of these relations is shown in Figure 5.

We use each one of these two LDR's to form a pair with the LDR of Section 3.1 and use the model relations of Figures 3 and 5 to search for a set of T_{eff} and $\log g$ which consistently fit the measurements of each of the two LDR's thus formed (*e.g.*, [VI/FeI, CaH/FeI] and [VI/FeI, CaH/VI]). For each pair of LDR's, a solution is found whenever the T_{eff}'s and $\log g$'s indicated by the LDR's disagree by less than 100K and $0.4dex$, respectively. We then take the average of the values given by each LDR. Hence, we have two determinations of T_{eff} and $\log g$ for each star: one obtained from the pair [VI/FeI, CaH/FeI] and the other from the pair [VI/FeI, CaH/VI]. We consider the solutions falling inside the range [3600,4400K], [2.5,4.5 *dex*] to be reliable. We find that the [VI/FeI, CaH/FeI] pair converges better than the other pair, in most cases, to a unique solution (*i.e.* T_{eff}'s and $\log g$'s as indicated by each LDR differing by less than 50K and $0.1dex$, respectively). This could be due to the fact the for stars cooler than 3900K, the VI line begins to saturate, which lowers the sensitivity of the CaH/VI LDR to both $\log g$ and T_{eff}.

We have observations on more than one night for AA, BP, DF and DK Tau. We can therefore check the stability of the LDR's against variations which may occur on timescales as short as one day. As mentioned in Section 2, the variations of LDR's in the spectra of AA Tau can not be accounted for by measurement errors alone. In fact, they are loosely correlated with veiling in the sense that data with larger veilings show "hotter" LDR's. Therefore, we choose the data with the best S/N and the lowest veiling in order to minimize the effect of any possible interference of disk accretion with the photospheric lines (see Batalha et al. 1995).

The final results are shown in Table 4 with superscripts *syn*. Both pairs yield the same result for AA Tau, BP Tau and CI Tau. The results of DE Tau, DF Tau and DK Tau are based solely on the [VI/FeI, CaH/FeI] pair. For V830 Tau, a consistent, but different, set of solutions converge for each LDR pair. Both are listed in Table 4. The uncertainties for this star are larger, given the low S/N of the spectrum and the relatively high $v\sin i$ ($\sim 25 km/s$). The results are displayed as points on Figure 5. There is a fair agreement between the T_{eff}'s determined by the LDR-pair method and those inferred from the intrinsic (R–I) colors, mainly for the stars with $\log g > 4.0$. This is because we used a calibration based on dwarf stars in

order to derive the intrinsic colors of the TTS. That calibration is expected to provide bluer colors for stars with lower gravities, because of the gravity dependence of the atomic LDR used (Figure 3). Indeed, for AA, CI and V830 Tau ($\log g \sim 3.8\ dex$), the T_{eff}^{c}'s exceed T_{eff}^{syn}'s by ~ 100K as shown in Table 4.

We do not find a set of atmospheric parameters satisfying the LDR measurements for ROX 6, GM Aur and DN Tau. We therefore compute $\log g$ for these stars by directly comparing the observed CaH lines with the synthetic ones, after proper veiling corrections are carried out (see Section 2). The synthetic spectra are computed following the procedure already described, and the adopted T_{eff}'s are derived from the intrinsic (R-I) colors. The chosen $\log g$ for each star is the one that gives the best fit to the observed CaH lines. The uncertainty involved in this method is larger, given the very high S/N it requires, and given the errors in the veiling and in the adopted $v\sin i$. ROX 6 has the largest uncertainty due to the poor S/N of its spectrum.

Because of the incompleteness of our atomic line list and the errors in the atomic oscillator strengths, the whole $\lambda\lambda$ 677.0-681.0 region is not well fitted by the synthetic spectra. Thus, we restrict the analysis to five sub-regions where blending is minimal, i.e., where Moore, Minnaert & Houtgast (1966) report no atomic lines. The fits are shown in Figure 6 and the gravities thus determined are shown in Table 4.

3.3 Comparing Previous Determinations of $\log g$

In order to compare our results to the data available in the literature, we compute surface gravities using luminosity and T_{eff} data from a number of authors. We locate each star on the H-R diagram and derive its gravity by interpolating among the theoretical evolutionary tracks from Cohen & Kuhi (1979). Spectral types (or temperatures, when available) and luminosities are from (Cohen & Kuhi 1979, Cohen, Emerson & Beichman 1988; Walter et al. 1988; Strom et al. 1989; Cabrit et al. 1990; Hartigan et al. 1991; Basri Martin & Bertout 1991, Magazzù, Rebolo & Pavlenko 1992). For those papers which only provide spectral types, we estimate the temperatures using the calibration of de Jager & Nieuwenhuijzen (1987). The resulting $\log g$'s are listed in Table 6. The spread among the values from various sources for some stars is quite striking. This is most likely due to the differing methods used to remove veiling (when done) and to correct for reddening. We also show the gravities obtained in the same way for the stars hotter than 4500K – T Tau, TAP 56 and UX Tau A – for which the CaH lines are too faint to provide any determination and the temperatures

were estimated from the calibration of Soderblom et al. (1993).

The agreement of our gravities with the ones from the literature is fairly good for AA, CI and V830 Tau. Our values tend to be above the average for the other stars. These differences can be partially explained in terms of the differences in the adopted temperatures. In order to test this hypothesis, we recompute the $\log g$ for these stars by placing them again in the HR diagram using our T_{eff}'s rather than the ones derived from the spectral types. The results are shown in Table 6, inside parentheses, for the stars whose T_{eff}'s as determined by us and other authors differ by 100K or more. We can see that, at least for DK Tau, DN Tau and GM Aur, the values inside parentheses are in good agreement with our $\log g$ determinations. We conclude that, for these stars, differences in $\log g$ can be reconciled by differences in assumed stellar temperatures.

For ROX 6, however, a large discrepancy remains – large enough that it cannot be explained even by luminosity errors in the work of Cohen & Kuhi (1979). As can be seen in Figure 6, there is significant noise in the CaH lines which implies that we are not confidently determining either the CaH line depth or the line shape, both basic to the successful aplication of the LDR method or direct synthesis. The cases of DE Tau and DF Tau are even more drastic, with discrepancies in $\log g$ of nearly 1 dex. It is likely that our values are overestimated since these stellar luminosities have been carefully measured (Strom et. al 1989) and they imply gravities lower than those we derive. As discussed previously, errors in the atomic and molecular data as well as in the adopted opacity sample are inherent in the theoretical LDR's and they certainly become larger at low temperatures. Furthermore, the contrast of the iron line at 5706 Å against the nearby continuum is severely decreased at temperatures lower than 3800 K. Thus, the line becomes inceasingly washed out by noise, especially in DE and DF Tau whose lines are already sizably veiled.

We conclude that the combined use of CaH with atomic lines to assess gravities and temperatures of TTS is efficient for temperatures in the range 4400 K – 3800 K. Table 5 provides a quick and easy assessment of the fundamental parameters of TTS with spectral types between K5 – M0. We foresee several improvements in our method such as: *i)* enlargement of the present set of line pairs, including others more efficient at temperatures lower than 3800 K; *ii)* inclusion of other hydride lines such as MgH in order to better constrain $\log g$. *iii)* Finally, future synthetic spectra will be more reliable if better atomic and molecular oscillator strengths, calibrated with a selected set of standards stars, are employed.

4. Summary

There is a growing need for spectral classification based on high resolution data, especially for young main sequence stars. We have derived temperatures and gravities of a small set of T Tauri stars, exploring the line depth ratio (LDR) technique, complemented by a spectral synthesis analysis of atomic and CaH rotational lines.

Temperatures are derived using an empirical relation between $(R–I)_0$ color indices and selected atomic LDRs of a set of template stars in the local field and the Hyades open cluster. Usually, TTS temperatures are derived from spectral types which are largely based on low dispersion spectra. Such analyses are subject to error due to the effects of veiling, metallicity, and the conversion between spectral type and T_{eff}. Our method is significantly less sensitive to veiling and metallicity, and therefore, produces more reliable temperature determinations.

At temperatures lower than 4400 K, we find a strong dependence of the LDR on gravity. The CaH lines are therefore included in the analysis in order to constrain $\log g$. This is accomplished by taking the ratio of the line depth of a rotational CaH line and two atomic lines. Computing theoretical relations between LDRs and T_{eff} and $\log g$ we derive a best value for each of these parameters.

For some stars, we are not able to find a pair of T_{eff} and $\log g$ which satisfies the LDR measurements. Their gravities are then obtained by fitting the observed CaH rotational lines with synthetic lines, adopting the T_{eff} derived from the intrinsic $(R–I)_0$ colors. The gravities derived for stars cooler than 3800K may be overestimated. The error can be mostly due to the low contrast between the iron line (5706 Å) and the local continuum. We conclude that the atomic line pair FeI/VI (5706/5707 Å) combined with the stronger CaH line here studied (6796 Å) yields an efficient and quick method to assess effective temperature and $\log g$ for TTS within the range $3800 < T_{eff} < 4400K$, being completely independent of veiling. We present the ne cessary calibration to derive these fundamental stellar parameters (Table 5) given the observed line depths.

In future work, additional observations of a larger number of standard stars and TTS with higher S/N are desirable in order to define new sets of LDRs and extend the method towards stars cooler than a typical M0 star. Likewise, it would be desirable to explore the rotational lines of MgH to confirm the values here derived and to refine the method. A study is being undertaken in order to calibrate the intensity of the near infrared FeH bands as a function of stellar parameters (Piorno Schiavon, Barbuy & Singh 1995, in preparation). Those bands are important gravity indicators for M-dwarf stars.

References

Balachandran, S. & Carr, J.: 1994, in "8th Cambridge Workshop on Cool Stars, Stellar Systems and the Sun", ed. J.-P. Caillaut.

Barbuy, B.: 1981, A&A, 101, 365.

Barbuy, B.: 1982, PhD. Thesis, Université de Paris, VII.

Barbuy, B., Schiavon, R.P., Gregorio-Hetem, J., Singh, P.D. and Batalha, C.: 1993, A&AS, 101, 409 (Paper I)

Basri, G. & Batalha, C.: 1990, ApJ, 363, 654.

Basri, G., Wilcots, E. and Stout, N.: 1989, PASP, 101, 528.

Basri, G., Martin, E.L., Bertout, C.: 1991, A&A, 252, 625 (BMB91)

Batalha, C.C. & Basri, G.: 1993, ApJ, 412, 363.

Batalha, C.C. et al.:1995 in preparation

Bell, R.A., Edvardsson, B. & Gustafsson, B.: 1985, MNRAS, 212, 497.

Bertout, C.: 1989, ARA&A, 27, 35.

Bertout, C., Basri, G., Bouvier, J.: 1988, ApJ, 330, 373

Bouvier, J.: 1990, AJ, 99, 946.

Boyer, R., Sotirovski, P. and Harvey, J.W.: 1975, A&AS, 19, 359.

Boyer, R., Sotirovski, P. and Harvey, J.W.: 1976, A&AS, 24, 111.

Boyer, R., Sotirovski, P. and Harvey, J.W.: 1978, A&AS, 33, 145.

Boyer, R., Sotirovski, P. and Harvey, J.W.: 1982, A&AS, 47, 145.

Cabrit, S., Edwards, S., Strom, S.E., Strom, K.M.: 1990, ApJ, 354, 687. (CESS)

Calvet, N., Basri, G. & Kuhi, L.V.: 1984, ApJ, 277, 725.

Calvet, N. & Marı n, Z.: 1987, Rev. Mex. Astr. Ap., 14, 353.

Cayrel de Strobel G., Hauck, B., François, P., Thévenin, F., Friel, E. Mermilliod, M., Borde, S.: 1992, A&AS, 95, 273.

Cohen, M., Emerson, J.P., Beichman, C.A.: 1988, ApJ, 339, 455 (CEB88)

Cohen, M., Kuhi, L.V.: 1979, ApJS, 41, 743 (CK79)

de Jager, C., Nieuwenhuijzen, H.: 1987, A&A, 177, 217

Delbouille, L., Roland, G., Neven, L.: 1973, "Photometric Atlas of the Solar Spectrum from 3000 to 10000 Å", Institut d'Astrophysique de Liège

Edwards, S., Hartigan, P., Shandon, L., Andrules: 1994, ApJ, accepted.

Finkenzeller, U., Basri, G.: 1987, ApJ, 318, 823.

Franchini, M., Castelli, F. & Stalio, R.: 1991, A&A, 241, 449.

Gliese, W.: 1969, Veröff. Astron. Rech. Inst., Heidelberg, 22.

Gray, D.F.: 1994, private comunication

Gray, D.F., Johanson, H.L.: 1991, PASP, 103, 439.

Griffin, R.F.: 1969, "A photometric atlas of the spectrum of Arcturus $\lambda\lambda 3600 - 8825\AA$", Cambridge Philosophical Society.

Hartigan, P., Hartmann, L., Kenyon, S.J., Hewett, R. and Stauffer, J.: 1989, ApJ, 70, 899.

Hartigan, P., Hartmann, L., Kenyon, S.J., Strom, S.E., Skrutskie, M.F.: 1990, ApJ, 354, L25.

Hartigan, P., Kenyon, S.J., Hartmann, L., Strom, S.E., Edwards, S., Welty, A.D. and Stauffer, J.: 1991, ApJ, 382, 617. (HKHSEWS).

Hartmann, L.W. & Kenyon, S.J.: 1987, ApJ, 349, 243.

Hartmann, L.W. & Kenyon, S.J.: 1990, ApJ, 349, 190.

Herbig, G.H. & Bell, K.R.: 1988, Lick Obs. Bull. 1111.

Holweger, H., Müller, E.: 1974, Solar Phys. 39, 19.

Kenyon, S.J., Hartmann, L. Hewett R., Carrasco, L. Cruz-Gonzalez, I., Recillas, E., Salas, L. & Serrano, A.: 1994, AJ, 107, 2153.

Königl, A.: 1991, ApJ, 370, L39.

Kurucz, R.L., Furenlid,I., Brault,J., Testerman,L.: 1984, "Solar Flux Atlas from 296 to 1300 nm "(Sunspot, N.M., National Solar Observatory).

Kurucz, R.: 1992, in IAU Symp. 149, 225

Magazzù, A., Rebolo, R., Pavlenko, Y.V.: 1992, ApJ, 392, 159. (MRP92)

Martin, E.L., Rebolo, R., Magazzù, A. & Pavlenko, Y.V.: 1994, A&A, 282, 503.

Moore, C.E., Minnaert, M.G.J. and Houtgast, J.: 1966, The "Solar Spectrum 2935Å to 8770Å" (Washington: National Bureau of Standards) (NBS Monograph 61).

Mould, J.R. & Wallis, R. E.: 1977, MNRAS, 181, 625.

Pallavicini, R., Cutispoto, G., Randich, S., Gratton, R.: 1993, A&A, 267, 145

Shu, F., Najita, J., Ostriker, E., Wilkin, F., Ruden, S. & Lizano, S.: 1994, ApJ, 429, 781.

Soderblom, D.R., Stauffer,J.R., Daniel Hudon, J. & Jones, B.F.: 1993, ApJS, 85, 315.

Strom, K.M., Strom, S.E., Kenyon, S.J. and Hartmann, L.: 1988, AJ, 95, 534.

Strom, K.M., Strom, S.E., Edwards, S., Cabrit, S., Skrutskie, M.F.: 1989, AJ, 97, 1451 (SSECS)

Upgren, A.R. .: 1974, ApJ, 193, 359.

Walter, F.M., Brown, A., Mathieu, R.D., Myers, P.C., Vrba, F.J.: 1988, AJ, 96, 297 (WBMMV)

Table 1 - Basic data for program stars

Star	Date	SpT	vsini(km/s)	veiling
AA Tau	12/22/86	K9	10	0.1
BP Tau	*average*	K7	< 10	
CI Tau	10/12/87	K6	11	0.1
DE Tau	10/12/87	M2	< 10	0.9
DF Tau	*average*	K7	10	
DK Tau	*average*	M0	10	
DN Tau	11/12/86	K7	10	0.0
GM Aur	10/11/87	K4	13	0.2
ROX 6	09/06/87	K5	< 10	0.3
T Tau	10/11/87	K2	20	0.1
TAP 56	11/29/88	K2	22	0.0
UX Tau A	12/22/86	K2	20	0.2
V830 Tau	11/12/86	K6	25	0.0

Table 2 - Basic data for template Hyades and field stars:

Star	Date	V	SpT	line ratio	$(R - I)_0$	$T_{\text{eff}}(K)$
HR1262	8/12/89	5.90	G5	0.48		
HR159	8/12/89	5.57	G8	0.60		
HR8	8/12/89	6.13	K0	0.64		
HR493	8/12/89	5.20	K1	0.83	0.29	5220
HR222	8/12/89	5.75	K2	0.92	0.33	5020
HR753	8/12/89	5.83	K3	1.13	0.36	4890
VA587	14/10/89	8.93	K0.5	0.76	0.31	5120
VA459	8/12/89	9.45	K2	0.87	0.34	4980
VA135	14/10/89	9.99	K4	1.14	0.47	4450
VA276	8/12/89	10.52	K5	1.32	0.49	4380
VA404	14/10/89	10.51	K7	1.71	0.63	4030
VA622	14/10/89	11.96	M0	2.23	0.69	3950

Table 3 - Line pair used in the temperature determination.

Species	λ(nm)	χ_{ex} (eV)	log gf
Fe1	570.601	4.61	-0.80
Fe1	570.611	4.28	-1.95
V1	570.698	1.04	-0.6
Fe1	570.705	3.64	-2.48

Table 4 - Line ratios, temperatures and gravities.

Name	line ratio	$(R-I)_0$	$T_{\mathrm{eff}}^{\mathrm{c}}$	$T_{\mathrm{eff}}^{\mathrm{syn}}$	$\log g^{\mathrm{syn}}$
AA Tau	2.02	0.67	3980	3840	3.9
BP Tau	1.77	0.63	4060	4100	4.3
CI Tau	1.42	0.54	4270	4200	3.8
DE Tau	3.04			3690	4.2
DF Tau	2.98			3660	4.0
DK Tau	1.39	0.51	4320	4260	4.2
DN Tau	1.68	0.61	4100		$3.8^{\dagger}$
GM Aur	1.18	0.47	4490		$4.5^{\dagger}$
ROX 6	1.34	0.52	4330		$4.2^{\dagger}$
T Tau	0.95	0.38	4870		
TAP 56	0.96	0.39	4860		
UX Tau A	0.93	0.38	4920		
V830 Tau	1.45	0.55	4240	$4010 - 4160$	$3.6 - 4.2$

Those values indicated by † were obtained from the synthesis of CaH lines. The others were obtained by interpolating the model relations between line depth ratios and $[T_{\mathrm{eff}}, \log g]$.

Table 5 - Line depth ratios computed from the synthetic spectra.

	V/Fe	CaH/Fe	CaH/V		V/Fe	CaH/Fe	CaH/V
		$\log g = 3.0$				$\log g = 4.0$	
$T_{eff}(K)$				$T_{eff}(K)$			
3600	2.04	1.94	0.81	3600	3.19	3.56	0.98
3800	1.68	0.95	0.51	3800	2.28	1.61	0.67
3900		0.65	0.39	3900		1.16	0.56
4000	1.44	0.50	0.32	4000	1.73	0.90	0.50
4100		0.32	0.22	4100		0.71	0.42
4200	1.28	0.19	0.14	4200	1.46	0.52	0.34
4300		0.12	0.09	4300		0.31	0.23
4400	1.18	0.06	0.05	4400	1.29	0.22	0.17
4500		0.02	0.02	4500		0.15	0.12
4600	1.08			4600	1.14		
4800	0.99			4800	1.02		
5000	0.91			5000	0.92		
5200	0.82			5200	0.82		
5400	0.72			5400	0.71		
5600	0.63			5600	0.62		
5800	0.54			5800	0.53		
		$\log g = 3.5$				$\log g = 4.5$	
$T_{eff}(K)$				$T_{eff}(K)$			
3600	2.45	2.56	0.91	3600	4.46	5.27	1.09
3800	1.88	1.28	0.60	3800	2.99	2.15	0.72
3900		0.90	0.48	3900		1.55	0.62
4000	1.56	0.71	0.41	4000	2.11	1.24	0.58
4100		0.50	0.32	4100		0.93	0.50
4200	1.36	0.33	0.23	4200	1.65	0.74	0.44
4300		0.19	0.15	4300		0.53	0.35
4400	1.22	0.11	0.08	4400	1.39	0.38	0.28
4500		0.06	0.05	4500		0.24	0.20
4600	1.10			4600	1.19		
4800	1.00			4800	1.03		
5000	0.92			5000	0.92		
5200	0.82			5200	0.81		
5400	0.72			5400	0.69		
5600	0.63			5600	0.60		
5800	0.54			5800	0.52		

Table 6 - Gravity values calculated using luminosity and T_{eff} data from the literature.

Star	CK79	CEB88	WBMMV	SSECS	CESS	HKHSEWS	BMB91	MRP92	This work
AA Tau	3.4	3.5		4.0	3.7	3.4/4.1	3.8		3.9
BP Tau	3.5	3.6		3.8	3.7	3.5/3.6	3.8	3.2	4.3
CI Tau	3.5	3.6(3.8)		3.8	4.0	3.6(3.8)	4.3(4.1)		3.8
DE Tau	3.1	3.4		3.3	3.5		3.4		4.2
DF Tau	2.8(2.6)	2.8(2.6)		3.2(3.1)	3.1(3.0)		3.0(3.0)		4.0
DK Tau	3.2(3.4)	3.4(3.7)		3.5(3.8)	3.6(3.8)	3.4(3.7)	3.5(3.8)		3.9
DN Tau	3.2(3.6)	3.2(3.6)		3.4(3.8)	3.4(3.8)	3.1(3.5)	3.7(3.8)		3.8
GM Aur	3.6(4.1)	3.5(4.1)		3.8(4.2)	3.6(4.1)		3.8(4.1)	3.4(4.1)	4.5
ROX 6	3.1(3.4)							3.0(3.4)	4.2
T Tau	3.0(3.1)	3.5(3.6)		3.3(3.4)	3.4(3.5)		3.6(3.5)		
TAP 56			3.8(4.0)				4.1(4.0)	3.6(4.0)	
UX Tau A	3.9(4.0)	4.2(4.2)		4.1(4.1)	4.2(4.2)		4.3(4.2)		
V830 Tau			3.7(3.9)				3.8		3.9

CK79: Cohen & Kuhi (1979)
CEB88: Cohen, Emerson & Beichman (1988)
WBMMV: Walter et al. (1988)
SSECS: Strom et al. (1989)
CESS: Cabrit et al. (1990)
HKHSEWS: Hartigan et al. (1991)

Captions to the Figures

● **Figure 1.** The line pair used in the T_{eff} determination, as seen in two Hyades stars of different spectral types, showing their inverse temperature sensitivity.

● **Figure 2.** The relation between line depth ratio and $(R-I)_{Kron}$, using template stars data (Table 2)

● **Figure 3.** Theoretical and observed relations between line ratio and effective temperature. Long dashes stand for $\log g = 4.5$, short dashes stand for $\log g = 4.0$, the dotted line stands for $\log g = 3.5$ and the full line stands for $\log g = 3.0$. The data are from the template stars listed in Table 2.

● **Figure 4.** Synthetic spectra showing the response of CaH lines to T_{eff} and $\log g$.

● **Figure 5.** Theoretical response of the line depth ratios (VI 570.7/FeI 570.6 nm and CaH 679.6/FeI 570.6 nm) to T_{eff} and $\log g$. The points show the final solutions for the program stars. The correspondence is the following: triangle-DE Tau, square-DF Tau, cross-AA Tau, asterisk-BP Tau, x-DK Tau, losangle-CI Tau

● **Figure 6.** Spectrum synthesis of rotational CaH lines for DN Tau, GM Aur and ROX 6.
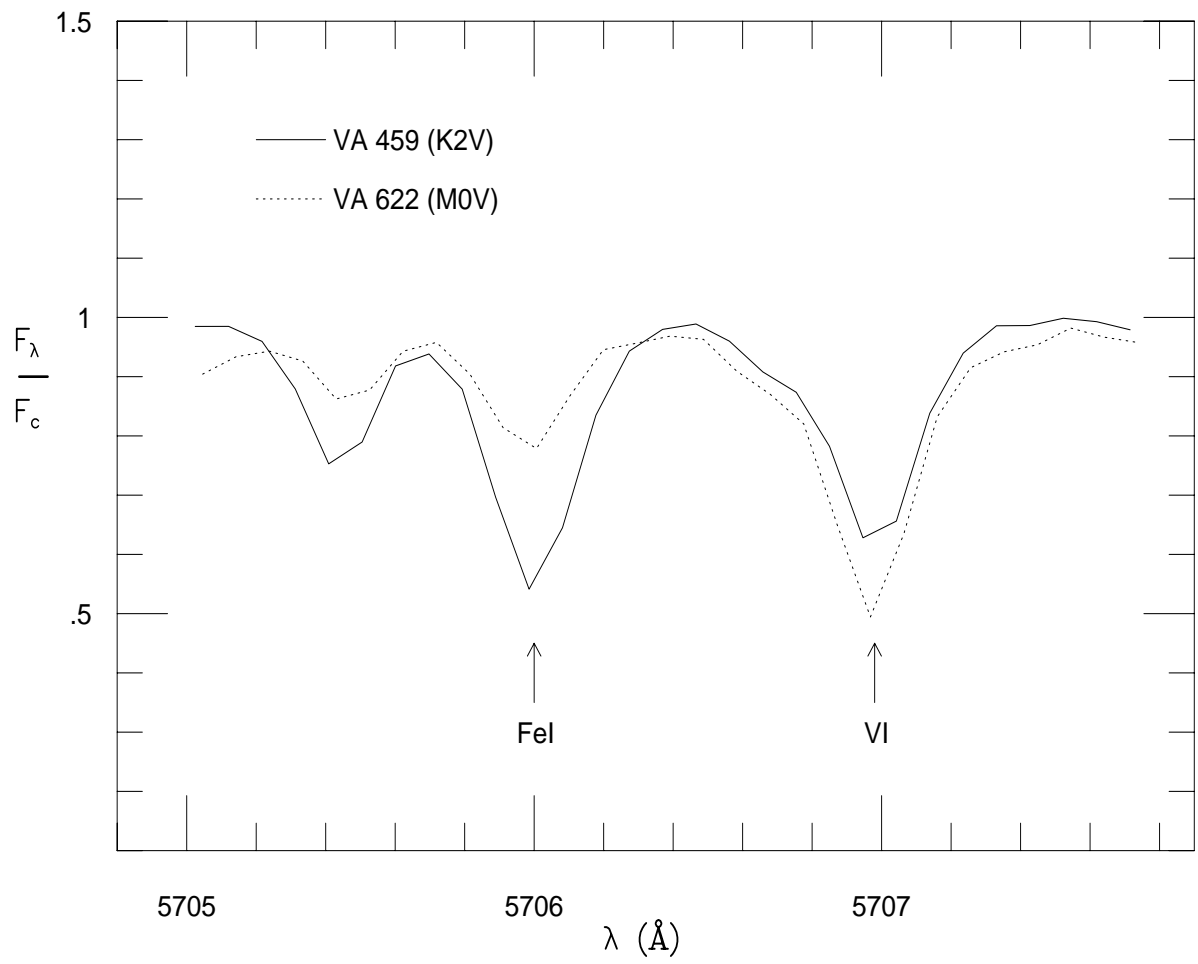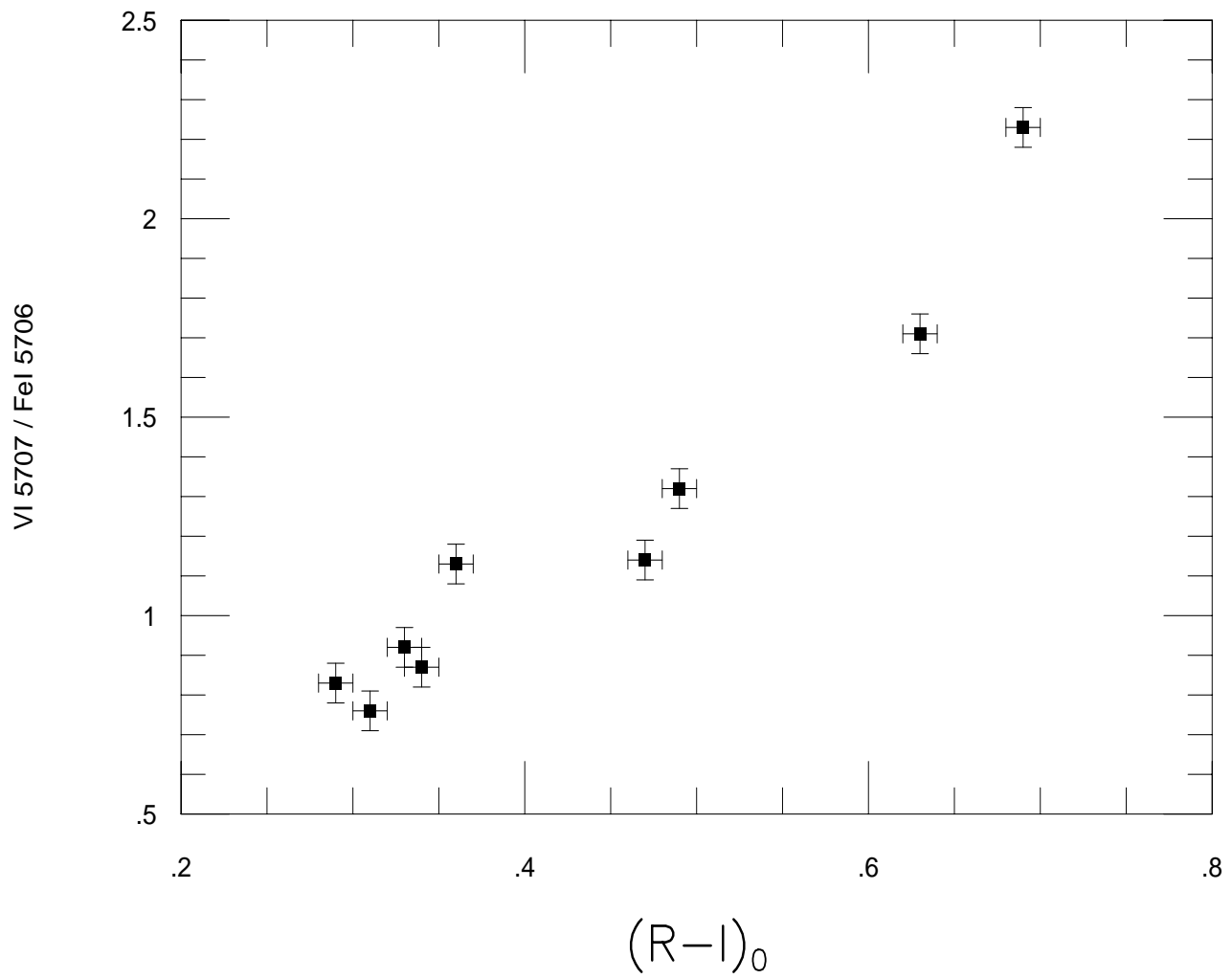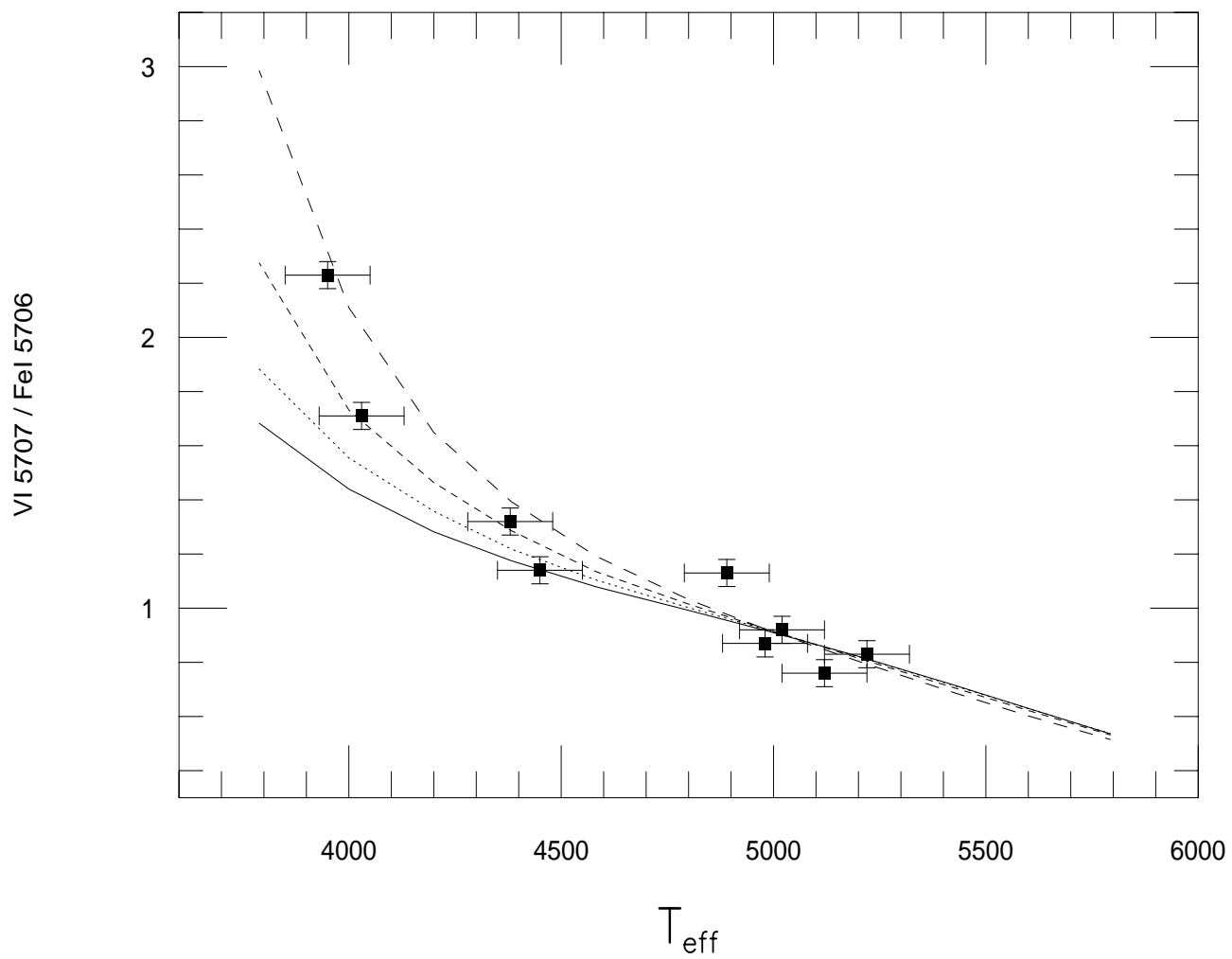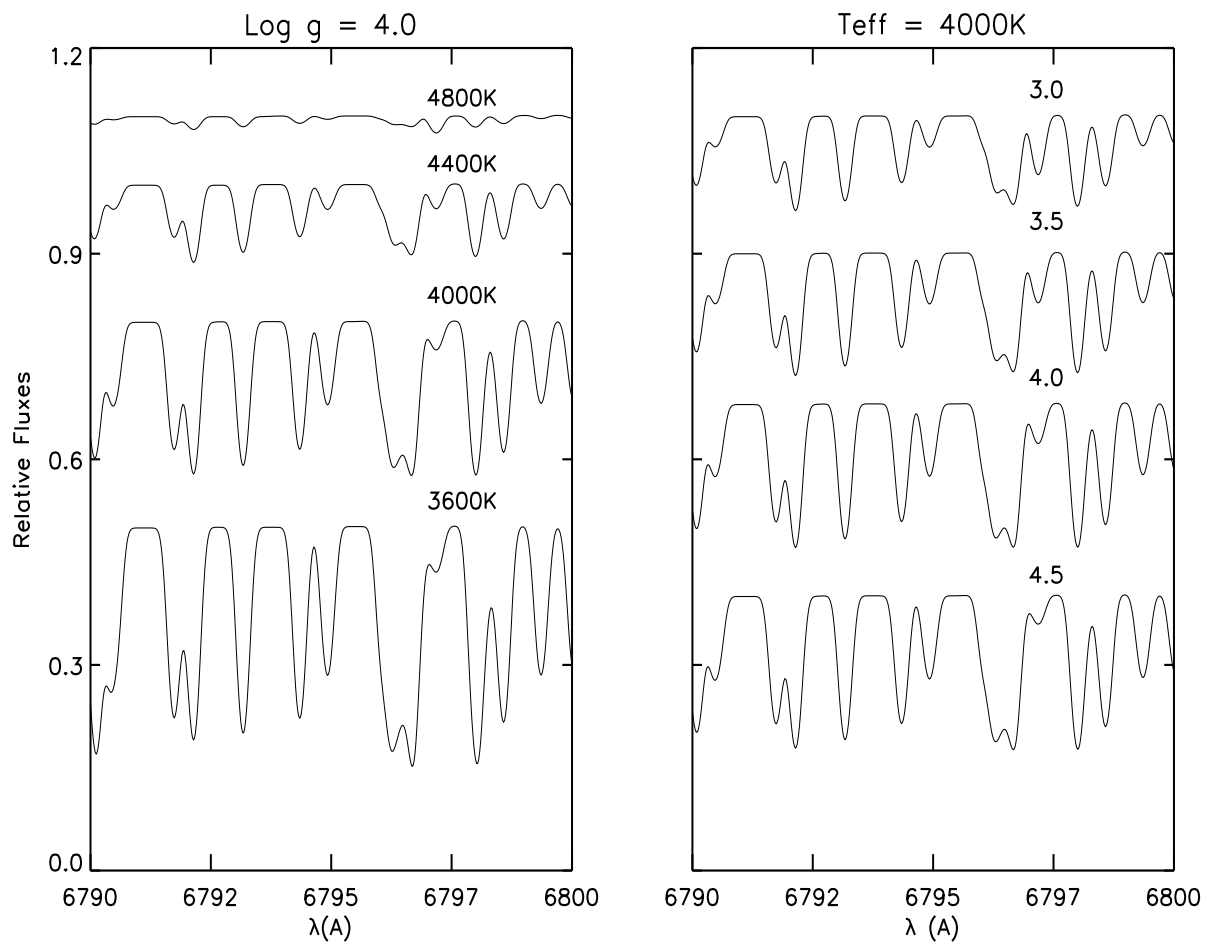
Figure 1.

Figure 2.

Figure 3.

Figure 4.
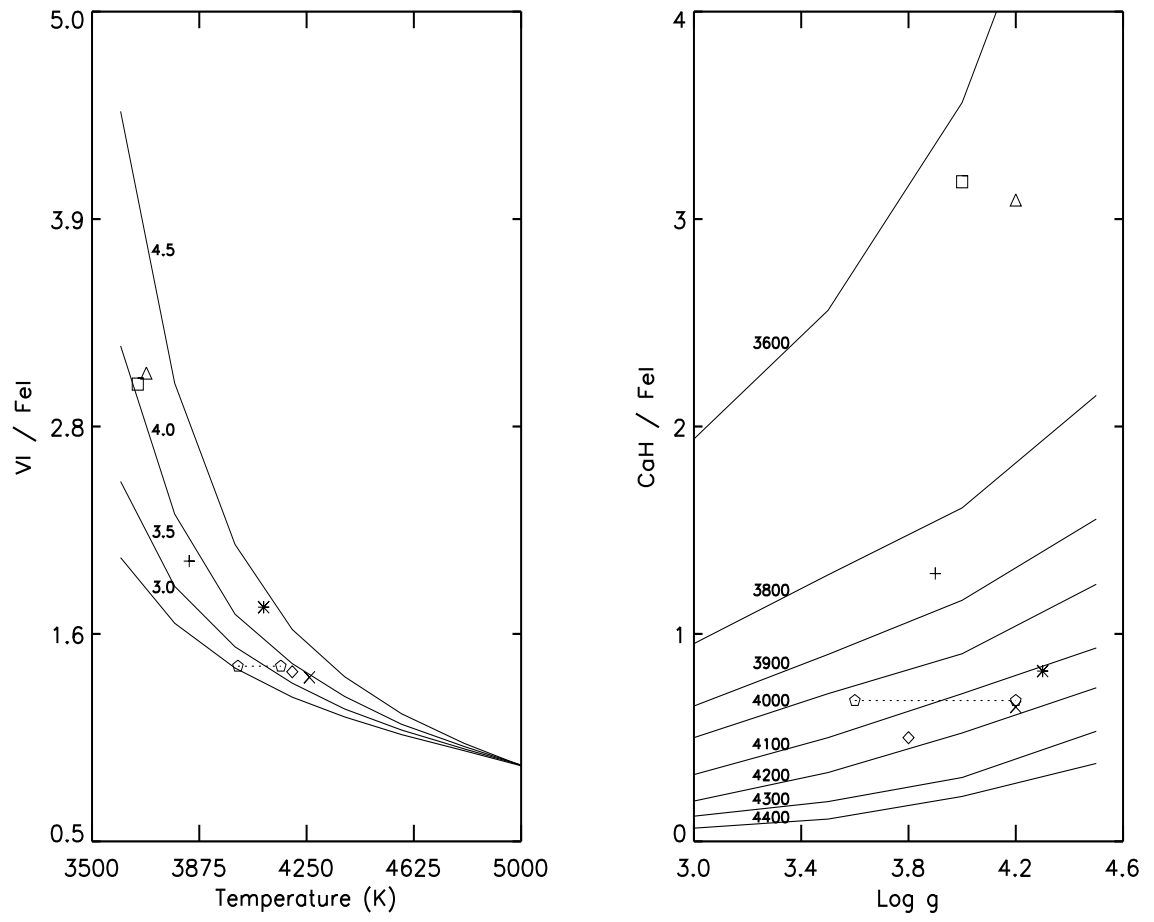
Figure 5.

Figure 6.

Figure 6. Cont.